

Chlorabietols A–C, Phloroglucinol-Diterpene Adducts from the Chloranthaceae Plant *Chloranthus oldhamii*

Juan Xiong,[†] Zhi-Lai Hong,[†] Li-Xin Gao,[‡] Jie Shen,[§] Shu-Ting Liu,[†] Guo-Xun Yang,[†] Jia Li,^{*,†} Huaqiang Zeng,[§] and Jin-Feng Hu^{*,†}

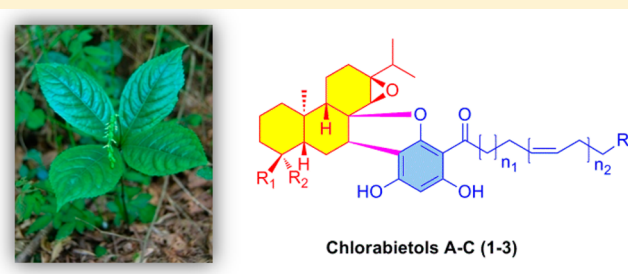
[†]Department of Natural Products Chemistry, School of Pharmacy, Fudan University, No. 826 Zhangheng Road, Shanghai 201203, P. R. China

[‡]State Key Laboratory of Drug Research, Shanghai Institute of Materia Medica, Chinese Academy of Sciences, No. 555 Zuchongzhi Road, Shanghai 201203, P. R. China

[§]Institute of Bioengineering and Nanotechnology, 31 Biopolis Way, The Nanos 138669, Singapore

Supporting Information

ABSTRACT: Three unprecedented phloroglucinol-diterpene adducts, chlorabietols A–C (1–3), were isolated from the roots of the rare Chloranthaceae plant *Chloranthus oldhamii*. They represent a new class of compounds, featuring an abietane-type diterpenoid coupled with different alkenyl phloroglucinol units by forming a 2,3-dihydrofuran ring. Their structures were elucidated by detailed spectroscopic analysis, molecular modeling studies, and electronic circular dichroism calculations. Compounds 1–3 showed inhibitory activity against protein tyrosine phosphatase 1B (PTP1B) with IC₅₀ values of 12.6, 5.3, and 4.9 μM, respectively.



The small plant genus *Chloranthus* (family Chloranthaceae) has less than 20 species worldwide.¹ The most abundant of these species have been chemically studied, and mono/disesquiterpenoids were found to be their characteristic secondary metabolites.² *C. oldhamii* Solms-Laub., usually found growing in damp, shady sites of mountain areas, is a rare species native to China.³ Because of the difficulty in collecting the samples, there has to date been no report of any chemical or pharmacological studies on this plant. As part of our ongoing research on the bioactive natural products from *Chloranthus* plants,⁴ the EtOH extract of the roots of *C. oldhamii* was phytochemically investigated, resulting in the isolation and characterization of chlorabietols A–C (1–3) (Figure 1). This class of compound contains an unprecedented skeleton, featuring an *ent*-abietane-type diterpenoid coupled with an alkenyl phloroglucinol moiety by forming an unexpected 2,3-dihydrofuran ring.

Meanwhile, four (4–7) possible biogenetic precursors of 1–3 (Figure 1) were also obtained. The ESI-MS, IR, UV, and NMR data (see Experimental Section) of 4 were all identical to those of known compound 4-*epi*-abietol (4a).⁵ However, 4 has a positive specific rotation ($[\alpha]_D^{25} +93$) in contrast with the negative one ($[\alpha]_D^{25} -135$)⁵ observed for 4a. Thus, 4 is regarded as the enantiomer of 4a. Actually, a number of *ent*-abietane-type diterpenoids have recently been reported from *Chloranthus sessilifolius*,⁴ a wild relative of the title plant. Compounds 5 and 7 were identified to be the known alkenyl phloroglucinols moniliferanone C⁶ and thouvenol B⁷, respectively. (*Z,Z,Z*)-1-(2',6'-Dihydroxy-4'-methoxyphenyl)-octade-

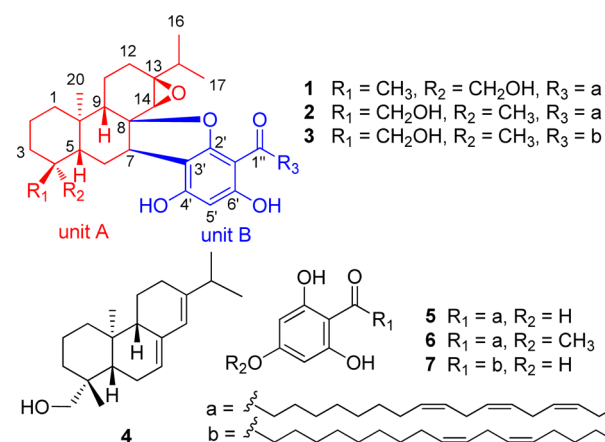


Figure 1. Structures of compounds 1–7.

ca-9,12,15-trien-1-one (6) is the 4'-methoxy derivative of 5, which was confirmed by spectroscopic data (see Experimental Section). Interestingly, naturally occurring C₂₄ acylphloroglucinols have been mainly obtained from the brown algae,^{6,8–10} and only a few have been previously reported from the terrestrial plant *Protorhus thouvenotii*.⁷ Thus, this is the first report regarding their occurrence in the *Chloranthus* genus. In this study, we present the isolation and structure elucidation of

Received: July 21, 2015

Table 1. ^1H and ^{13}C NMR Data for **1** and **2** in CDCl_3

no.	1		2		no.	1		2	
	δ_{H} , m (J in Hz)	δ_{C}	δ_{H} , m (J in Hz)	δ_{C}		δ_{H} , m (J in Hz)	δ_{C}	δ_{H} , m (J in Hz)	δ_{C}
1 α	1.76, m	41.0	1.68, m	39.9	1'		101.9		102.8
1 β	0.90, m		0.89, dd (12.3, 12.0)		2'		160.7		161.4
2 β	1.58, m	18.3	1.59, m	17.8	3'		108.3		107.3
2 α	1.43, m		1.49, m		4'		159.7		158.9
3 α	1.81, br d (13.7)	35.1	1.19, br d (10.8)	35.2	5'	5.87, s	96.5	5.88, s	96.9
3 β	0.89, m		1.50, dd (12.0, 10.8)		6'		165.2		165.0
4		38.1		37.6	1''		204.3		204.3
5 β	1.21, br d (12.8)	49.0	1.42, br d (12.9)	41.0	2''	3.01, dt (15.1, 7.8)	42.9	2.99, dt (15.1, 7.8)	43.0
6 β	2.42, br d (13.8)	22.7	2.47, br d (14.7)	20.7		2.88, dt (15.1, 7.5)		2.90, dt (15.1, 7.9)	
6 α	1.78, m		1.76, ddd (14.7, 12.9, 5.2)		3''	1.66, m	24.4	1.66, m	24.1
7 α	3.71, br d (6.0)	44.3	3.71, br d (5.2)	46.6	4''	1.33, m	29.3	1.33, m	29.3
8		91.8		92.7	5''	1.33, m	29.5	1.33, m	29.4
9 β	1.65, overlap	53.6	1.66, overlap	51.6	6''	1.33, m	29.6	1.33, m	29.7
10		36.4		37.3	7''	1.33, m	29.7	1.33, m	29.7
11 α	1.98, m	21.9	1.96, m	21.6	8''	2.06, m	27.3	2.06, m	27.3
11 β	1.96, m		2.04, br d (12.0)		9''	5.38, m	130.3	5.38, m	130.3
12	1.33, 2H, m	29.7	1.33, 2H, m	29.7	10''	5.31, m	127.1	5.31, m	127.1
13		64.5		64.0	11''	2.81, t (6.6)	25.6	2.82, t (6.0)	25.6
14 α	2.93, s	62.9	3.03, s	62.3	12''	5.36, m	128.2	5.36, m	128.2
15	1.58, m	34.1	1.58, m	34.5	13''	5.36, m	128.3	5.36, m	128.3
16	1.02, d (6.8)	17.6	1.05, d (7.2)	17.5	14''	2.81, t (6.6)	25.5	2.82, t (6.0)	25.5
17	0.95, d (6.8)	18.1 ^c	0.98, d (7.2)	18.0	15''	5.35, m	127.8	5.33, m	127.7
18	0.88, s	26.9	3.60, d (11.7)	71.8	16''	5.41, m	132.0	5.40, m	132.0
			3.03, d (11.7)						
19	3.88, d (10.7)	65.2	0.80, s	18.0	17''	2.08, m	20.5	2.07, m	20.5
	3.52, d (10.7)				18''	0.98, t (7.5)	14.3	0.98, t (7.5)	14.3
20	0.97, s	17.3	1.09, s	16.8	6'-OH	13.5, s		13.4, s	

1–**3** as well as the inhibitory effects of compounds **1**–**7** on protein tyrosine phosphatase 1B (PTP1B).

Chlorabietol A (**1**) showed a $[\text{M} + \text{H}]^+$ ion peak at m/z 689.4767 in its positive mode HR-ESI-MS, corresponding to the molecular formula $\text{C}_{44}\text{H}_{64}\text{O}_6$ (calcd 689.4776). The strong absorption bands (ν_{max}) in its IR spectrum denoted the presence of hydroxy (3397 cm^{-1}) and conjugated carbonyl (1618 cm^{-1}) groups in **1**. By analysis of the ^{13}C NMR data (Table 1) of **1**, with the aid of DEPT and HSQC experiments, forty-four carbon signals were identified consisting of five methyls, 17 methylenes (one oxygenated), 12 methines (one oxygenated), nine quaternary carbons (two oxygenated), and one carbonyl group.

In the ^1H NMR spectrum (Table 1) of **1**, characteristic signals for a hydroxymethyl group with an ABq system [δ 3.88 and 3.52 (each 1H, d, $J = 10.7\text{ Hz}$), H₂-19], two doublet [δ 1.02 and 0.95 (each 3H, d, $J = 6.8\text{ Hz}$), Me-16 and Me-17], and two singlet [δ 0.97 (Me-20) and 0.88 (Me-18)] methyls were observed. The above proton signals together with their corresponding carbon resonances are strongly reminiscent of an *ent*-abietanol skeleton similar to **4**⁵ (Figure 1), which was confirmed by interpretation of its COSY and HMBC spectra (Figure 2). In particular, the proton resonating at δ 2.93 (1H, s, H-14) and carbons at δ 62.9 (C-14) and 64.5 (C-13) suggested a 13,14-epoxide ring,¹¹ which was verified by the HMBC correlations from H-7 to C-14, from H-14 to C-7/C-8/C-9/C-13/C-15, and from Me-16/Me-17 to C-13/C-15.

Among the remaining 24 carbon signals attributed to unit B, seven signals resonating at δ_{C} 204.3 (C-1''), 165.2 (C-6'), 160.7 (C-2'), 159.7 (C-4'), 108.3 (C-3'), 101.9 (C-1'), and 96.5 (C-5'), along with a singlet aromatic proton at δ_{H} 5.87 (H-5') and

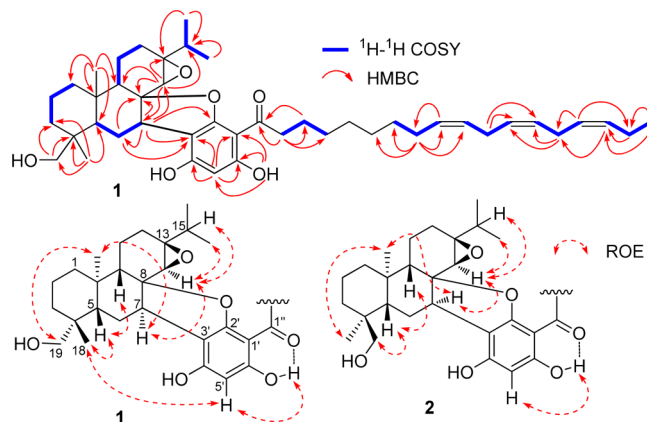


Figure 2. Selected COSY, HMBC, and/or ROE correlations of **1** and **2**.

a broad singlet at δ_{H} 13.5 (6'-OH, D_2O exchangeable) in the ^1H NMR spectrum of **1**, were typical of an acylphloroglucinol moiety.^{6–9} A linear C_{17} alkene with three double bonds was thereafter elucidated based on the remainder of the carbon signals: one methyl at δ_{C} 14.3, ten sp^3 methylenes at δ_{C} 20.5–42.9, and six well-resolved olefinic carbons at δ_{C} 127.1, 127.8, 128.2, 128.3, 130.3, and 132.0 (Table 1). The three double bonds in the side chain all adopted the *Z* geometry because the six olefinic proton signals (δ_{H} 5.29–5.43) are narrowed.⁹ This was supported by the upfield ^{13}C NMR resonances for the two bisallylic methylene carbons [δ_{C} 25.6 (C-11'') and 25.5 (C-14'')] and the two allylic carbons [δ_{C} 27.3 (C-8'') and 20.5 (C-17'')], which were in full agreement with

those of reported resorcinols with two or more *Z*-configured double bonds in their alkenyl units.^{7,9} These NMR data were superimposable on those of moniliferanone C (**5**) just isolated from the brown algae *Cystophora subfarcinata*.⁶ The planar structure of unit B was then verified to be the same as **5** by further COSY and HMBC experiments (Figure 2).

By now, the above units A and B accounted for 11 out of the 12 degrees of unsaturation in **1**. The remaining one degree of unsaturation and the unusual chemical shifts of H-7 (δ_{H} 3.71, br d), C-7 (δ_{C} 44.3, d), and C-8 (δ_{C} 91.8, s) suggested that the phloroglucinol moiety was coupled to the diterpene unit at C-7 and C-8. The linkage positions were further confirmed through the HMBC experiment (Figure 2) and corroborated by ab initio calculations¹² (Figures S1 and S2 in the Supporting Information). Clear HMBC correlations were observed between H₂-6 and C-3' (δ_{C} 108.3) and between H-7 and C-3'/C-2' (δ_{C} 160.7) (Figure 2). On the basis of the above evidence, units A and B should be conjugated by forming a 2,3-dihydrofuran ring, which was constructed via either C(7)-C(3')/C(8)-O-C(2') or C(7)-C(3')/C(8)-O-C(4') bonds. Molecular modeling was utilized to determine which possibility was more likely. For simplification of the computation, the flexible polyene chain in **1** was replaced by a methyl group. Therefore, a simplified structure **1a** and the most possible isomers (**1b**, **1c**, **1d**) (Figure S1) were used for ab initio calculations. As presented in Figure S2, **1a** is the most potential stable inequivalent configuration (0 kcal/mol) among the diastereomers. The calculated relative energies for the two conformers of **1c** (**1c**₁ and **1c**₂) are 2.14 and 7.01 kcal/mol, respectively, suggesting **1c**₁ to be preferred over **1c**₂ [i.e., $\Delta E(\mathbf{1c}_1-\mathbf{1c}_2) > 3$ kcal/mol implied a ratio of >99:1 (**1c**₁/**1c**₂)].¹³ Because **1b** and **1d** are much less stable than their respective stereoisomers **1a** and **1c**₁ by more than 19 kcal/mol, they can be ruled out. Thus, only **1a** and **1c**₁ resulted in stable structures at room temperature. Of these, **1c**₁ could be readily excluded by the diagnostic HMBC correlations from H-5' to C-1'/C-3'/C-4'/C-6' and from the hydrogen-bonded -OH (δ_{H} 13.5) to C-1'/C-5'/C-6' (Figure 2 and Figure S1).

The relative configuration of **1** was determined by analyses of the proton coupling constants (Table 1) and ROESY data (Figure 2). The large *J* value (12.8 Hz) observed for H-5 and a smaller one (6.0 Hz) for H-7 revealed that H-5 adopted the axial position, whereas H-7 was equatorial. Clear ROE correlations of H₂-19/Me-20, Me-20/H-7, H-7/H-14, and H-14/H-15 indicated these protons in the same orientation. In contrast, ROE correlations of Me-18/H-5 and H-5/H-9 suggested they were cofacial. Additionally, a clear ROE relation between H-5' and Me-18 was only consistent with the corresponding calculated ¹H-¹H interproton distances in **1a** (4.53/5.03/5.95 Å, Table S1). This strongly supported the aforementioned structure assignment for compound **1**.

The stereochemistry of complex structure **1**, especially the configuration of C-8, would be better determined by single crystal X-ray diffraction analysis. However, growing crystals was not achieved in the present study, probably due to the flexibility of the linear chain. Nevertheless, the configuration of C-8 could be assumed by ab initio calculations (Figures S1 and S2).¹² As described above, a supposed 8-epimeric structure (**1b**) of **1a** exerted a much higher relative energy than **1a** ($\Delta E = 21.43$ kcal/mol), indicating that the 2,3-dihydrofuran ring should orient as *cis* to the diterpene unit. The absolute configurations at C-7 and C-8 in **1** were determined by comparison of the experimental and calculated electronic circular dichroism

(ECD) spectra.¹⁴ As shown in Figure 3, the experimental ECD spectrum of **1** overlapped well with the calculated ECD of

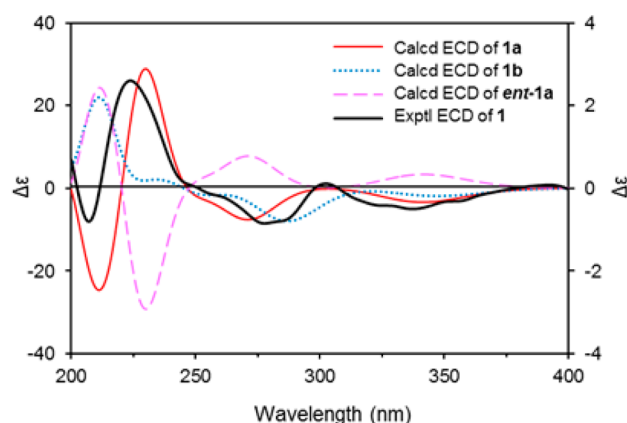


Figure 3. Experimental ECD spectrum of **1** and calculated ECD of **1a**, **1b**, and *ent*-**1a** in MeOH.

1a but was rather different from those of the 8-epimer (**1b**) and enantiomer (*ent*-**1a**, Figure S3) of **1a**, which unequivocally suggested an absolute configuration of 4*R*,5*S*,7*R*,8*R*,9*S*,10*R*,13*S*,14*R* for compound **1**.

Chlorabietol B (**2**) was assigned the same molecular formula as that of **1** by its HR-ESI-MS data. Likewise, the two compounds have almost identical ¹H and ¹³C NMR data (Table 1) except for those in the vicinity of C-4. The obvious upfield shift of C₄-Me (δ_{C} 26.9 in **1**, 18.0 in **2**) and a downfield shift of -CH₂OH (δ_{C} 65.2 in **1**, 71.8 in **2**) were observed, indicating **2** possesses a different configuration at C-4. This was further verified by the ROESY data. The ROE correlations of Me-19/Me-20, Me-20/H-7, H-7/H-14, H-14/H-15, H-14/Me-17, H₂-18/H-5, and H-5/H-9 established the relative configuration of **2** as shown in Figure 2. Similar Cotton effects observed for **2** ($\Delta\epsilon_{223} +4.16$, $\Delta\epsilon_{280} -1.36$) and **1** ($\Delta\epsilon_{223} +2.60$, $\Delta\epsilon_{277} -0.85$) in their ECD spectra (Figure S4) indicated that they shared the same absolute configuration of (7*R*,8*R*). Thus, the entire structure (4*S*,5*S*,7*R*,8*R*,9*S*,10*R*,13*S*,14*R*) of chlorabietol B (**2**) was determined as depicted.

The NMR data (Table 2) of **3** closely resembled those of **2**, but slight differences were observed among the polyene side chain. In the ¹H NMR spectrum of **3**, the olefinic signals between δ_{H} 5.32–5.42 integrated only for four protons, together with its molecular formula C₄₄H₆₆O₆ established by its HR-ESI-MS data, indicating one less double bond in the side chain than that of **2**. The two double bonds in the C₁₇ alkenyl chain of **3** were then established to be at $\Delta^{10''}$ and $\Delta^{13''}$ by detailed inspection of the HMBC correlations (Figure S5). Similar to **1**, both the two double bonds in the side chain have the *Z* geometry according to the ¹³C NMR chemical shifts of the bisallylic methylene carbon C-12'' (δ_{C} 25.6) and the two allylic carbons C-9'' (δ_{C} 27.2) and C-15'' (δ_{C} 27.2).^{7,9} Actually, the NMR spectroscopic data of unit B in **3** were found to be in full agreement with those of thouverol B⁷ (**7**, Figure 1). As expected, subsequent analyses of the coupling constants, ROE correlations, and experimental ECD data (Figure S4) revealed that **3** has the same absolute configuration as that of **2**.

Compounds **1**–**7** were tested for their inhibitory activity against PTP1B, a promising drug target for type II diabetes and obesity.^{15,16} As shown in Table 3, the isolates bearing an alkenyl phloroglucinol moiety all exhibited inhibitory effects with IC₅₀

Table 2. ^1H and ^{13}C NMR Data for **3** in CDCl_3

unit A			unit B		
no.	δ_{H} , m, (J in Hz)	δ_{C}	no.	δ_{H} , m, (J in Hz)	δ_{C}
1 α	1.68, m	39.9	1'		102.8
1 β	0.89, m		2'		161.4
2 β	1.59, m	17.9	3'		107.1
2 α	1.49, m		4'		158.7
3 α	1.19, br d (10.8)	35.1	5'	5.89, s	96.9
3 β	1.50, m		6'		165.0
4		37.6	1''		204.3
5 β	1.42, br d (12.5)	40.9	2''	3.00, dt (15.1, 7.8)	43.1
6 α	1.76, m	20.6		2.90, dt (15.1, 7.7)	
6 β	2.46, br d (14.7)		3''	1.67, m	24.0
7 α	3.72, br d (5.0)	46.6	4''	1.34, m	29.3
8		92.7	5''	1.34, m	29.3
9 β	1.66, overlap	51.6	6''	1.34, m	29.4
10		37.3	7''	1.34, m	29.7
11 α	1.96, m	21.6	8''	1.34, m	29.7
11 β	2.04, br d (12.0)		9''	2.06, m	27.2
12	1.33, 2H, m	29.7	10''	5.41, m	130.1
13		64.0	11''	5.38, m	130.2
14 α	3.03, s	62.3	12''	2.81, t (6.6)	25.6
15	1.58, m	34.5	13''	5.36, m	128.0
16	1.05, d (7.0)	17.6	14''	5.33, m	127.9
17	0.99, d (7.0)	18.0	15''	2.06, m	27.2
18	3.60, d (11.9)	71.7	16''	1.34, m	31.5
	3.03, d (11.9)		17''	1.36, m	22.6
19	0.80, s	18.0	18''	0.89, t (6.8)	14.1
20	1.09, s	16.8	6'-OH	13.3, s	

Table 3. Inhibitory Effects of **1–7** on PTP1B

compound	IC_{50} (μM)	compound	IC_{50} (μM)
1	12.6 \pm 0.7	5	8.1 \pm 0.5
2	5.3 \pm 0.4	6	16.2 \pm 1.4
3	4.9 \pm 0.4	7	3.8 \pm 0.4
4	>20	oleanolic acid	3.2 \pm 0.2

values in the range of 3.8–16.2 μM . Oleanolic acid¹⁶ was used as the positive control. In contrast, diterpene **4** was inactive (IC_{50} > 20 μM), suggesting that the alkenyl phloroglucinol moiety would be essential for such potent inhibitory activities of chlorabietols A–C.

In summary, the present phytochemical investigation on the rare plant *C. oldhamii* led to the discovery of a novel class of phloroglucinol-diterpene adducts (**1–3**). To our knowledge, the phloroglucinol-coupled monoterpenes and sesquiterpenes have often been found from the Myrtaceae family.^{14,17} However, the occurrence of phloroglucinol-diterpene adducts from natural sources has never been reported until the present study. Bioassay results indicated these unique phloroglucinol-diterpene adducts to be potential leads of antidiabetic drugs.

EXPERIMENTAL SECTION

General Experimental Procedures. Optical rotations were measured on a digital polarimeter. The UV spectrum was recorded by a spectrophotometer using MeOH as the solvent. The IR spectrum was measured by an IR spectrometer with KBr disks. ECD spectra were taken on a spectropolarimeter. NMR spectra were obtained on 400 and 500 MHz spectrometers. Chemical shifts are expressed in δ (ppm) and referenced to the residual solvent signals. NMR peak assignments are based on ^1H – ^1H COSY, HSQC, and HMBC spectroscopic data. ESI-MS were measured on a quadrupole-based

API mass spectrometer, and HR-ESI-MS was performed on a triple-TOF mass spectrometer fitted with an ESI source. An HPLC pump coupled to a photodiode array detector (PAD) and an evaporative light-scattering detector (ELSD), and either a Fluophase PFP column (5 μm , 250 \times 7.7 mm, flow rate: 2.0 mL/min) or an ODS column (5 μm , 250 \times 10 mm, flow rate: 3.0 mL/min), were utilized for the semipreparative HPLC separations. Column chromatography (CC) was performed using silica gel (200–300 mesh), MCI gel (75–150 μm), and LH-20. Silica gel-precoated plates (GF254, 0.25 mm) were used for TLC detection. Spots were visualized using UV light (254 and/or 365 nm) and by spraying with 15% $\text{H}_2\text{SO}_4/\text{EtOH}$ followed by heating to 120 $^\circ\text{C}$.

Plant Material. The roots of *C. oldhamii* were collected in July 2011 from the Jinggang Mountains, Jiangxi Province of China. The plant was identified by Prof. Zhensheng Yao (Zhejiang Chinese Medical University). A voucher specimen (No. 20110701) was deposited at the Herbarium of the Department of Natural Products Chemistry, School of Pharmacy at Fudan University.

Extraction and Isolation. Dried roots of *C. oldhamii* (7.0 kg) were pulverized and extracted with 95% EtOH at room temperature three times (3 \times 10 L). After filtration, the solvents were removed under vacuum to give a crude extract (550 g, semidry), which was suspended in H_2O (1.0 L) and then partitioned successively with petroleum ether (2 \times 1.0 L) and EtOAc (3 \times 1.0 L). After removal of solvent, the entire EtOAc extract (71.5 g) was fractionated by silica gel CC using petroleum ether (PE)/EtOAc in a gradient (20:1 to 0:1, v/v) and then MeOH to give 16 fractions (Fr. 1–Fr. 16). Fraction 5 (5.0 g) was rechromatographed on silica gel (PE/EtOAc 15:1 to 5:1, v/v; PE/ CH_2Cl_2 3:1, v/v) to afford **4** (30.5 mg, yield: 0.0004%), which was further purified by gel permeation chromatography (GPC) on Sephadex LH-20 (MeOH). Fraction 7 (2.0 g) was subjected to an MCI gel column eluted with MeOH/ H_2O (8:2 to 10:0, v/v) to give six subfractions, Fr. 7.1–7.6. Subfraction 7.4 (215.4 mg) was separated by gel permeation chromatography (GPC) on Sephadex LH-20 (MeOH) and further purified by RP-C18 HPLC using MeOH- H_2O (93:7, v/v)

as the eluting solvent to yield compound **6** (103.2 mg, $t_R = 22.3$ min, yield: 0.0015%). Fraction 11 (4.1 g) was also fractionated by CC over MCI gel using MeOH-H₂O (8:2 to 10:0, v/v) and nine fractions (Fr. 11.1–11.9) were collected. Fraction 11.7 (330.6 mg) was subjected to further RP-C18 HPLC purification using an isocratic elution of 93% MeOH-H₂O (v/v) to afford compounds **5** (220.0 mg, $t_R = 13.3$ min, yield: 0.003%) and **7** (16.1 mg, $t_R = 18.9$ min, yield: 0.0002%). Subsequent separation of fraction 11.9 (356.4 mg) by CC over silica gel (CH₂Cl₂/MeOH 25:1) and then Sephadex LH-20 (MeOH) gave compounds **2** and **3** as a mixture, which were successfully separated by semipreparative HPLC using a Thermo Fluophase PFP column (MeOH/H₂O 90:10, v/v; 2: 14.2 mg, $t_R = 22.9$ min, yield: 0.0002%; 3: 3.4 mg, $t_R = 25.4$ min, yield: 0.00005%). Fraction 13 (1.7 g) was loaded on a Sephadex LH-20 column with MeOH to give nine fractions, Fr. 13.1–13.9. Subfraction 13.8 (260.0 mg) was decolorized by an MCI gel column with MeOH/H₂O (8:2 to 10:0, v/v) and further purified by RP-C18 HPLC using MeOH/H₂O (98:2, v/v) to furnish compound **1** (6.3 mg, $t_R = 29.5$ min, yield: 0.00009%).

Chlorabietol A (1). White amorphous powder; $[\alpha]_D^{25} +43.1$ (c 0.51, MeOH); UV (MeOH) λ_{max} (log ϵ) 231 (3.76), 285 (3.73) nm; ECD (c 9.6×10^{-4} M, MeOH) λ_{max} ($\Delta\epsilon$) 223 (+2.60), 277 (−0.85) nm; IR (film) ν_{max} 3397 (OH), 3009 (C=C–H), 2962, 2927, 2854, 1618 (C=O), 1507, 1431, 1372, 1262, 1184, 1017, 896, 821, 716, and 679 cm^{−1}; ¹H and ¹³C NMR data, see Table 1; (+) ESI-MS m/z 689 [M + H]⁺, 711 [M + Na]⁺; (+) HR-ESI-MS m/z 689.4767 [M + H]⁺ (calcd for C₄₄H₆₅O₆, 689.4776, $\Delta = -1.2$ ppm).

Chlorabietol B (2). White amorphous powder; $[\alpha]_D^{25} +18.7$ (c 0.08, MeOH); UV (MeOH) λ_{max} (log ϵ) 232 (3.34), 284 (3.15) nm; ECD (c 7.3×10^{-4} M, MeOH) λ_{max} ($\Delta\epsilon$) 223 (+4.16), 280 (−1.36) nm; IR (film) ν_{max} 3400, 3011, 2962, 2924, 2852, 1620, 1507, 1432, 1374, 1262, 1183, 1017, 822, 723, and 680 cm^{−1}; ¹H and ¹³C NMR data, see Table 1; (+) ESI-MS m/z 689 [M + H]⁺, 711 [M + Na]⁺; (−) ESI-MS m/z 687 [M–H][−]; (−) HR-ESI-MS m/z 687.4615 [M–H][−] (calcd for C₄₄H₆₃O₆, 687.4625, $\Delta = -1.5$ ppm).

Chlorabietol C (3). White amorphous powder; $[\alpha]_D^{25} +11.6$ (c 0.06, MeOH); UV (MeOH) λ_{max} (log ϵ) 232 (3.50), 284 (3.33) nm; ECD (c 4.3×10^{-4} M, MeOH) λ_{max} ($\Delta\epsilon$) 224 (+2.66), 280 (−1.34) nm; IR (film) ν_{max} 3400, 3010, 2962, 2920, 2854, 1619, 1521, 1457, 1376, 1258, 1184, 1015, 820, 718, and 690 cm^{−1}; ¹H and ¹³C NMR data, see Table 1; (+) ESI-MS m/z 691 [M + H]⁺, 711 [M + Na]⁺; (−) ESI-MS m/z 689 [M–H][−]; (−) HR-ESI-MS m/z 689.4778 [M–H][−] (calcd for C₄₄H₆₅O₆, 689.4781, $\Delta = -0.4$ ppm).

19-Hydroxy-ent-abieta-7,13-diene (4). Colorless oil; $[\alpha]_D^{25} +92.6$ (c 0.08, CHCl₃); UV (MeOH) λ_{max} (log ϵ) 241 (3.21) nm; IR (film) ν_{max} 3424, 2962, 2927, 2867, 1654, 1561, 1459, 1383, and 1028 cm^{−1}; ¹H NMR (in CDCl₃) δ 5.78 (1H, s, H-14), 5.41 (1H, t, $J = 2.5$ Hz, H-7), 3.90 (1H, d, $J = 11.0$ Hz, H-19a), 3.52 (1H, d, $J = 11.0$ Hz, H-19b), 2.24 (1H, m, H-15), 2.20 (1H, m, H-6 β), 2.08 (2H, m, H-9 and H-12a), 1.98 (1H, m, H-6 α), 1.89 (1H, br d, $J = 12.7$ Hz, H-1 α), 1.88 (1H, m, H-12b), 1.85 (1H, m, H-3 α), 1.50 (2H, m, H₂-2), 1.47 (1H, dd, $J = 12.6, 4.0$ Hz, H-5), 1.46 (1H, m, H-11a), 1.24 (1H, m, H-11b), 1.12 (1H, br ddd, $J = 12.8, 12.6, 4.5$ Hz, H-3 β), 0.97 (1H, m, H-1 β), 1.02 (3H, d, $J = 6.9$ Hz, CH₃-17), 1.01 (3H, d, $J = 6.9$ Hz, CH₃-16), 0.95 (3H, s, CH₃-18), 0.78 (3H, s, CH₃-20); ¹³C NMR (in CDCl₃) δ 39.3 (C-1), 18.5 (C-2), 35.8 (C-3), 37.9 (C-4), 51.1 (C-5), 23.5 (C-6), 121.1 (C-7), 135.4 (C-8), 51.3 (C-9), 34.8 (C-10), 22.8 (C-11), 27.5 (C-12), 144.9 (C-13), 122.5 (C-14), 34.8 (C-15), 20.8 (C-16), 21.4 (C-17), 26.7 (C-18), 64.7 (C-19), 14.6 (C-20); (+) ESI-MS m/z 289 [M + H]⁺, 311 [M + Na]⁺; (+) HR-ESI-MS m/z 289.2519 [M + Na]⁺ (calcd for C₂₀H₃₃O, 289.2526, $\Delta = -2.5$ ppm).

(Z,Z,Z)-1-(2',6'-Dihydroxy-4'-methoxyphenyl)-octadeca-9,12,15-trien-1-one (6). White amorphous powder; UV (MeOH) λ_{max} (log ϵ) 226 (3.93), 283 (4.02) nm; IR (film) ν_{max} 3415, 3010, 2928, 2854, 1630, 1587, 1520, 1426, 1390, 1208, 1161, 1079, 822, and 722 cm^{−1}; ¹H NMR (in CDCl₃) δ 5.94 (2H, s, H-3/H-5), 5.30–5.39 (6H, m, H-9'/H-10'/H-12'/H-13'/H-15'/H-16'), 3.79 (3H, s, OMe), 3.07 (2H, m, H₂-2'), 2.82 (4H, t, $J = 6.0$ Hz, H₂-11'/H₂-14'), 2.09 (2H, m, H₂-17'), 2.05 (2H, m, H₂-8'), 1.69 (2H, m, H₂-3'), 1.34 (8H, m, H₂-4'–H₂-7'), 0.98 (3H, t, $J = 7.6$ Hz, CH₃-18'); ¹³C NMR (in CDCl₃) δ 104.9 (C-1), 163.3 (C-2), 94.3 (C-3), 165.4 (C-4), 94.3 (C-5), 163.3

(C-6), 206.2 (C-1'), 44.0 (C-2'), 24.6 (C-3'), 29.2 (C-4'), 29.4 (C-5'), 29.6 (C-6'), 29.6 (C-7'), 27.2 (C-8'), 130.4 (C-9'), 127.1 (C-10'), 25.6 (C-11'), 128.3 (C-12'), 128.3 (C-13'), 25.5 (C-14'), 127.7 (C-15'), 132.0 (C-16'), 20.5 (C-17'), 14.3 (C-18'), 55.5 (OMe); (+) ESI-MS m/z 401 [M + H]⁺, 423 [M + Na]⁺; (+) HR-ESI-MS m/z 401.2692 [M + H]⁺ (calcd for C₂₅H₃₇O₄, 401.2686, $\Delta = 1.3$ ppm).

ECD Calculations. The ECD spectra of compounds **1a**, **1b**, and **ent-1a** were calculated according to the protocols as described previously.¹⁴ For details, see Supporting Information.

PTP1B Inhibitory Activity Assay. The inhibitory activities of all samples against PTP1B were tested according to a previously described procedure with slight modifications.¹⁶ The recombinant GST-hPTP1B (glutathione S-transferase-human protein tyrosine phosphatase 1B) was obtained from *Escherichia coli* BL21 expression system. The enzymatic activities of the PTP1B catalytic domain were determined at 30 °C by monitoring the hydrolysis of *para*-nitrophenyl phosphate (*p*-NPP). The dephosphorylation *p*-NPP of generates product *p*-NP, which could be monitored at an absorbance of 405 nm by the VersaMax microplate reader (Molecular Devices, USA). All samples were dissolved in dimethyl sulfoxide (DMSO), and reactions were performed at a final concentration of 1% DMSO. Oleonic acid (purity $\geq 98\%$) was used as the positive control. In a typical 100 μ L assay mixture containing 50 mM 3-[*N*-morpholino]-propanesulfonic acid (MOPS), pH 6.5, 2 mM *p*-NPP, and 30 nM recombinant PTP1B, activities were continuously monitored, and the initial rate of the hydrolysis was determined using the early linear region of the enzymatic reaction kinetic curve. The IC₅₀ was calculated with Prism 4 software (GraphPad Software, San Diego, CA) from the nonlinear curve fitting of the percentage of inhibition (% inhibition) versus the inhibitor concentration [I] by using the following equation: % inhibition = 100/[1 + (IC₅₀/[I])^k], where *k* is the Hill coefficient.

■ ASSOCIATED CONTENT

Supporting Information

The Supporting Information is available free of charge on the ACS Publications website at DOI: 10.1021/acs.joc.5b01658.

Ab initio calculation, ECD calculations, and copies of MS and 1D/2D NMR spectra (PDF)

■ AUTHOR INFORMATION

Corresponding Authors

*E-mail: jli@sim.ac.cn.

*E-mail: jfhu@fudan.edu.cn.

Notes

The authors declare no competing financial interest.

■ ACKNOWLEDGMENTS

This work was financially supported by NSFC grants (21472021, 81273401, and 81202420) and the National Basic Research Program of China (973 Program, Grant 2013CB530700). The authors thank Dr. Courtney Starks (Sequoia Sciences, Ins., USA) for her valuable suggestions, and Dr. Shou-De Zhang (School of Pharmacy, East China University of Science and Technology, China) for his assistance with the ECD calculations.

■ REFERENCES

- (1) Editorial committee. *Flora of China* (Zhongguo Zhiwu Zhi); Science Press: Beijing, 1982; Vol. 20, p 81.
- (2) Wang, A.-R.; Song, H.-C.; An, H.-M.; Huang, Q.; Luo, X.; Dong, J.-Y. *Chem. Biodiversity* **2015**, *12*, 451–473.
- (3) (a) Editorial committee. *Flora of China* (Zhongguo Zhiwu Zhi); Science Press: Beijing, 1982; Vol. 20, p 84. (b) Zhang, H.-Y.; Zhang, Z.-Y. *Essential Records of Resources in Chinese Materia Medica* (Zhongguo Zhongyao Ziyuan Zhiyao); Zeng, M.-Y., Zeng, J.-F., Eds.; Science Press: Beijing, 1994; p 392.

- (4) Wang, L.-J.; Xiong, J.; Liu, S.-T.; Pan, L.-L.; Yang, G.-X.; Hu, J.-F. *J. Nat. Prod.* **2015**, *78*, 1635–1646.
- (5) (a) Tabacik, C.; Poisson, C. *Phytochemistry* **1971**, *10*, 1639–1645.
(b) Mossa, J. S.; Muhammad, I.; El-Ferally, F. S.; Hufford, C. D. *Phytochemistry* **1992**, *31*, 2789–2792.
- (6) Brkljača, R.; Urban, S. *Phytochemistry* **2015**, *117*, 200–208.
- (7) Cao, S.; Schilling, J. K.; Randrianasolo, A.; Andriantsiferana, R.; Rasamison, V. E.; Kingston, D. G. I. *Planta Med.* **2004**, *70*, 683–685.
- (8) Gregson, R. P.; Kazlauskas, R.; Murphy, P. T.; Wells, R. J. *Aust. J. Chem.* **1977**, *30*, 2527–2532.
- (9) (a) Kazlauskas, R.; King, L.; Murphy, P. T.; Warren, R. G.; Wells, R. J. *Aust. J. Chem.* **1981**, *34*, 439–447. (b) Barrow, R. A.; Capon, R. J. *Aust. J. Chem.* **1991**, *44*, 1393–1405.
- (10) (a) Reddy, P.; Urban, S. *J. Nat. Prod.* **2008**, *71*, 1441–1446.
(b) Laird, D. W.; Bennett, S.; Bian, B.; Sauer, B.; Wright, K.; Hughes, V.; van Altena, I. A. *Biochem. Syst. Ecol.* **2010**, *38*, 187–194.
- (11) (a) Valverde, S.; Lopez, J. C.; Rabanal, R. M.; Escudero, J. *Tetrahedron* **1986**, *42*, 573–582. (b) Ohtsu, H.; Tanaka, R.; In, Y.; Matsunaga, S.; Tokuda, H.; Nishino, H. *Planta Med.* **2001**, *67*, 55–60.
- (12) Wu, S.-B.; Bao, Q.-Y.; Wang, W.-X.; Zhao, Y.; Xia, G.; Zhao, Z.; Zeng, H.; Hu, J.-F. *Planta Med.* **2010**, *76*, 1–7.
- (13) Lodewyk, M. W.; Siebert, M. R.; Tantillo, D. J. *Chem. Rev.* **2012**, *112*, 1839–1862.
- (14) Wang, J.; Zhai, W.-Z.; Zou, Y.-K.; Zhu, J.-J.; Xiong, J.; Zhao, Y.; Yang, G.-X.; Fan, H.; Hamann, M. T.; Xia, G.; Hu, J.-F. *Tetrahedron Lett.* **2012**, *53*, 2654–2658.
- (15) (a) Combs, A. P. *J. Med. Chem.* **2010**, *53*, 2333–2344.
(b) Johnson, T. O.; Ermolieff, J.; Jirousek, M. R. *Nat. Rev. Drug Discovery* **2002**, *1*, 696–709.
- (16) Liang, L.-F.; Kurtán, T.; Mándi, A.; Yao, L.-G.; Li, J.; Zhang, W.; Guo, Y.-W. *Org. Lett.* **2013**, *15*, 274–277.
- (17) Singh, I. P.; Bharate, S. B. *Nat. Prod. Rep.* **2006**, *23*, 558–591.